The Canadian Mineralogist
Vol. 38, pp. 45-56 (2000)

MORPHOLOGY OF JAROSITE-GROUP COMPOUNDS PRECIPITATED FROM BIOLOGICALLY AND CHEMICALLY OXIDIZED Fe IONS

KEIKO SASAKI§

Laboratory of Environmental Science, Otaru University of Commerce, Otaru 047-8501, Japan

HIDETAKA KONNO

Graduate School of Engineering, Hokkaido University, Sapporo 060-8628, Japan

Abstract

Jarosite-group compounds [$MFe_3(SO_4)_2(OH)_6$: argentojarosite ($M^+ = Ag^+$), jarosite ($M^+ = K^+$), ammoniojarosite ($M^+ = NH_4^+$)] were synthesized by supplying Fe^{3+} ions in three different ways: biological oxidation of Fe^{2+} ions by *T. ferrooxidans* (biological products), chemical oxidation of Fe^{2+} ions by slow addition of H_2O_2 (chemical products 1), and chemical oxidation by rapid addition of H_2O_2 (chemical products 2). These were characterized by XRD, FTIR, chemical analysis and SEM; as well, the morphological features were compared with those formed by the hydrothermal method (standard substances). The jarosite-group compounds so synthesized do not contain crystalline by-products, as revealed by XRD, but the order of purity inferred from IR spectra, which is determined by the intensity of specific peaks, was found to be dependent on the method of preparation and is independent of the jarosite species; the order was found to be standard substances > chemical products 2 > chemical products 1 > biological products. Two main factors were found to affect the morphology, the method and rate of supply of Fe^{3+} ions to the system and the nature of the monovalent cations, which determine the intrinsic rate of formation under given conditions. Where Fe^{3+} ions are present in the system from the beginning, the order of rate of formation is confirmed to be argentojarosite > jarosite > ammoniojarosite at 30°C. Morphological features of jarosite-group phases formed by the biological method were rendered distinguishable by the effect of extracellular substances. Morphological information is useful to distinguish the mode of occurrence of jarosite-group phases in natural samples, since it may be difficult to do so by other analytical techniques, such as XRD, FTIR, Raman spectroscopy and chemical analysis.

Keywords: argentojarosite, jarosite, ammoniojarosite, morphology, *Thiobacillus ferrooxidans*, oxidation rate of Fe^{2+} ions, precursor.

Sommaire

Les composés du groupe de la jarosite [$MFe_3(SO_4)_2(OH)_6$: argentojarosite ($M^+ = Ag^+$), jarosite ($M^+ = K^+$), et ammoniojarosite ($M^+ = NH_4^+$)] ont été synthétisés en ajoutant les ions Fe^{3+} de trois façons différentes: oxydation biologique d'ions Fe^{2+} par la participation de *T. ferrooxidans* (produits biologiques), oxydation chimique des ions Fe^{2+} par addition lente de H_2O_2 (produits chimiques 1), et oxydation chimique par addition rapide de H_2O_2 (produits chimiques 2). On a caractérisé ces produits par diffraction X, par spectroscopie infra-rouge avec transformation de Fourier, par analyse chimique et par microscopie électronique à balayage. De plus, les aspects morphologiques ont été comparés avec ceux des produits de synthèse hydrothermale (étalons). Les composés du groupe de la jarosite ainsi synthétisés ne contiennent pas d'autres produits cristallins, comme le prouve la diffraction X. En revanche, la séquence de pureté, d'après les spectres infra-rouges, déterminée à partir de l'intensité d'absorptions spécifiques, dépend du mode de préparation et non de l'espèce de composé. Cette séquence serait: étalons > produits chimiques 2 > produits chimiques 1 > produits biologiques. Deux facteurs régissent la morphologie des particules, le mode de formation et le taux d'addition des ions Fe^{3+} au système et la nature des cations monovalents, qui détermine le taux intrinsèque de formation à des conditions spécifiées. Lorsque les ions Fe^{3+} sont présents dans le système dès le début, le taux de formation diminue selon la séquence argentojarosite > jarosite > ammoniojarosite à 30°C. Les caractéristiques morphologiques des phases du groupe de la jarosite formées par la méthode biologique ont pu être distinguées grâce à l'effet de substances extracellulaires. L'information à propos de la morphologie est très utile pour distinguer le mode d'origine des phases du groupe de la jarosite dans les échantillons naturels, vue la grande difficulté de les distinguer par les autres méthodes d'analyse, par exemple diffraction X, spectroscopie infra-rouge, spectroscopie de Raman et analyse chimique.

(Traduit par la Rédaction)

Mots-clés: argentojarosite, jarosite, ammoniojarosite, morphologie, *Thiobacillus ferrooxidans*, taux d'oxydation des ions Fe^{2+}, précurseur.

§ *E-mail address*: keikos@res.otaru-uc.ac.jp

INTRODUCTION

Jarosite-group minerals [$M_nFe_3(SO_4)_2(OH)_6$, where M is a monovalent or divalent cation, and n is 1 or 1/2] commonly occur as secondary minerals in acidic and sulfate-rich environments, such as acid mine-drainage. Therefore, they are good indicators of strongly acidic environments, whereas goethite (α-FeOOH) and schwertmannite [$Fe_8O_8(OH)_6SO_4$] are ultimate products of pyrite weathering in weakly acidic or neutral environments (Nordstrom 1982, Taylor *et al.* 1984, Lazaroff *et al*. 1982, Bigham 1994, Akai *et al.* 1999).

It is well known that the iron-oxidizing bacteria (mainly *Thiobacillus ferrooxidans*) actively grow in mine environments and play an important role in the formation of acid mine-drainage (Singer & Stumm 1970). Thermophilic bacteria, such as *Acidanus briery,* are also suggested to be indirectly involved in the formation of jarosite in hydrothermal chimney fragments of black smoker (Verati *et al.* 1999). There has been some debate concerning the way the acidophilic bacteria take part in the formation of jarosite: do they contribute to the crystallization of jarosite and, in addition, to the oxidation of Fe^{2+} ions? Sasaki *et al.* (1995) have reported the formation of argentojarosite in the presence of *T. ferrooxidans* and concluded that neither *T. ferrooxidans* itself nor extracellular substances make any direct contribution to crystallization of argentojarosite. Our group found, however, that biologically mediated products commonly form aggregates, probably because of extracellular substances, such as secretions from cells. Sadowski (1999) has reported that polysaccharide causes an increase of the adhesion of microbial cells and jarosite particles. Jarosite ($M^+ = K^+$), natrojarosite ($M^+ = Na^+$), ammoniojarosite ($M^+ = NH_4^+$), and argentojarosite ($M^+ = Ag^+$) have been formed experimentally in the presence of *T. ferrooxidans,* and the morphology of the products has been reported by several investigators (Lazaroff *et al.* 1985, Grishin *et al.* 1988, Koiwasaki *et al*. 1993, Sasaki *et al.* 1995, Sasaki 1997). On the other hand, which factors control the morphology of jarosite-group phases has not been fully discussed. The process of formation of natural jarosite is roughly explained by three steps: the oxidation of Fe^{2+} to Fe^{3+} ions, the formation of crystal nuclei (embryo), and the growth of crystals of a jarosite-group phase. Therefore, it is probable that several factors affect the morphology of jarosite-group minerals. The morphological information is important in order to understand the environment in which jarosite-group phases occur.

In the present work, argentojarosite [$AgFe_3(SO_4)_2(OH)_6$], jarosite [$KFe_3(SO_4)_2(OH)_6$], and ammoniojarosite [$NH_4Fe_3(SO_4)_2(OH)_6$] were synthesized by 1) mediation of biological agents, with chemical oxidation of Fe^{2+} to Fe^{3+} ions, and 2) providing Fe^{3+} ions initially. The morphological development of the precipitates are compared and discussed.

MATERIALS AND METHODS

Formation of jarosite-group compounds

Method I is a simple preparation made by heating the appropriate "alkali" sulfate with $Fe_2(SO_4)_3 \cdot xH_2O$ to temperatures near the solution's boiling point. Details have been reported elsewhere (Dutrizac & Kaiman 1976). The jarosite, ammoniojarosite, and argentojarosite synthesized by this method were supplied by Dr. J.E. Dutrizac at CANMET, Canada, and used as standard substances for our spectroscopic analyses. The composition of these phases is shown in Table 1.

Method II involves the biologically mediated formation of jarosite-group phases using Fe^{3+} ions oxidized from Fe^{2+} ions by *T. ferrooxidans*. Jarosite-group compounds were formed in light-shielded 500 cm^3 Erlenmeyer flasks with gas-permeable plugs (silico plug) containing 150 cm^3 of 160 mmol dm^{-3} $FeSO_4 \cdot 7H_2O$, adjusted to a pH of 2.2 using H_2SO_4 and Li_2CO_3. Lithium ions are not structurally incorporated in jarosite-type compounds (Dutrizac & Kaiman 1976). We used a strain of *Thiobacillus ferrooxidans* (HUTY 8906) that was isolated from acid drainages in the Toyoha mines, Hokkaido, Japan (Sasaki *et al.* 1993), and cultivated conventionally in 150 cm^3 of 9K medium (Silverman & Lundgren 1959) adjusted to a pH of 2.0 with H_2SO_4 using 500 cm^3 Erlenmeyer flasks capped with gas-permeable plugs (Sasaki *et al.* 1995). Inoculation size was 2×10^8 cells/flask. The flask was incubated on a rotary shaker for 56 days at 30°C. Under such conditions, bacteria cannot grow fully because of a lack of N and P sources. After the oxidation of Fe^{2+} ions was complete, which was confirmed by spectrophotometry with 1,10-phenanthroline, stoichiometric amounts of $AgNO_3$, K_2SO_4, or $(NH_4)_2SO_4$ were added to the solution ([M^+] = 53.3 mmol dm^{-3}). The precipitate was aged for 168 hours in the incubator under the same conditions. Cells were killed by the addition of Ag^+ ions, which was confirmed by microscopy and the termination of bacterial motion. The critical dose of Ag^+ ions is reported to be around 10^{-5} mol dm^{-3} (Sugio *et al.* 1981). The precipitate for characterization was collected by filtration with a 0.20 μm Millipore filter, air-dried, and kept in a desiccator at room temperature. Hereafter, this sample is denoted the "biological product."

Method III involves chemical formation using Fe^{3+} ions oxidized by H_2O_2. First, 6.672 g of $FeSO_4 \cdot 7H_2O$ was dissolved into 50 cm^3 of H_2SO_4 (pH 2.00) in a 500 cm^3 Erlenmeyer flask. Then, 100 cm^3 of 0.42% H_2O_2 was added using a peristaltic pump to the flask at 0.7 cm^3 min^{-1} to slowly oxidize Fe^{2+} ions at 30°C, giving a final pH of 2.10. Addition of Ag^+, K^+, or NH_4^+ ions and aging for precipitation were carried out as with Method II. An experiment with the rapid addition of 100 cm^3 of 0.42% H_2O_2 was also carried out, and the precipitate was collected and kept in the same manner as above.

TABLE 1. COMPOSITION, COLOR, SPECIFIC SURFACE-AREA, FWHM*1 OF THE 113 XRD PEAK AND UNIT-CELL PARAMETERS FOR BIOLOGICALLY AND CHEMICALLY PRODUCED ARGENTOJAROSITE, JAROSITE AND AMMONIOJAROSITE

Sample	Elemental composition M Fe S / wt% (mole ratio M:Fe:S)	Color*2	S_{BET} /m^2g^{-1}	FWHM of 113 XRD peak/ 2θ	Lattice parameter *a*/nm	*c*/nm
argentojarosite (M^+= Ag^+): JCPDS 41-1398					7.35	16.58
Standard	17.3 29.8 11.9 (1: 3.31: 2.33)	5.0Y 8.5/11	2.7_1	0.106	7.35	16.55
Biological	14.6 29.1 11.2 (1: 3.71: 2.50)	5.0Y 8.5/11	1.7_4	0.111	7.35	16.56
Chemical 1 (slow)	15.5 31.4 11.7 (1: 3.93: 2.55)	5.0Y 8.5/11	1.2_5	0.097	7.35	16.55
Chemical 2 (rapid)	14.5 29.6 11.1 (1: 3.95: 2.58)	5.0Y 8.5/11	1.4_6	0.106	7.35	16.57
jarosite (M^+= K^+): JCPDS 36-427					7.29	17.22
Standard	5.49 30.0 13.6 (1: 3.86: 3.03)	5.0Y 8.5/11	4.0_7	0.160	7.29	17.14
Biological	5.22 30.8 13.4 (1: 4.12: 3.13)	5.0Y 8.5/11	1.1_0	0.18	7.29	17.06
Chemical 1 (slow)	4.84 31.0 14.6 (1: 4.96: 3.98)	5.0Y 9.0/7	1.1_5	0.18	7.31	17.12
Chemical 2 (rapid)	3.93 27.8 12.8 (1: 4.48: 3.69)	5.0Y 9.0/7	0.6_5	0.18	7.28	17.12
ammoniojarosite (M^+= NH_4^+): JCPDS 26-1014					7.33	17.50
Standard	3.46 33.8 42.1 (1: 2.71: 2.23)	5.0Y 9.0/7	3.8_6	0.13	7.33	17.58
Biological	14.6 29.1 11.2 (1: 4.06: 2.89)	5.0Y 8.5/11	0.9_0	0.16	7.28	17.42
Chemical 1 (slow)	15.5 31.4 11.7 (1: 3.15: 2.41)	5.0Y 8.5/11	0.9_1	0.18	7.31	17.45
Chemical 2 (rapid)	14.5 29.6 11.1 (1: 3.80: 2.59)	2.0Y 8.0/14	0.5_8	0.17	7.33	17.45

*1 full width at half maximum
*2 expressed by JIS symbols.

Hereafter, the sample prepared by the slow addition is denoted "chemical product 1" and that by rapid addition, "chemical product 2".

Method IV also involved chemical formation, but $Fe_2(SO_4)_3 \cdot xH_2O$ was used instead of oxidizing Fe^{2+} to Fe^{3+} ions. This was carried out to determine the rate of formation of the jarosite-group compounds. The 120 cm^3 of 100 mmol dm^{-3} $Fe_2(SO_4)_3 \cdot xH_2O$ was put into a 500 cm^3 Erlenmeyer flask, and then $AgNO_3$, K_2SO_4, or $(NH_4)_2SO_4$ were added to the flask in order for the final concentration to be $[M^+]_{final}$ = 53 mmol dm^{-3}, where M^+ indicates a monovalent cation such as Ag^+, K^+, or NH_4^+. Finally, 30 cm^3 of H_2O was added. The final pH was adjusted to 1.90–2.00 using Li_2CO_3. Aging for precipitation was continued for 56 days at 30°C. At intervals, pH was measured, and 1 cm^3 of supernatant was pipetted off and filtered with a 0.20 μm membrane filter for solution analysis. The total Fe and S concentrations were determined by the induced coupled plasma – atomic emission spectrometry, ICP–AES (SEIKO Co. Ltd., SPS 1200) after dilution with a 0.01 mol dm^{-3} super special grade (SSG) of HCl solution. After aging the precipitate, the residue was separated by filtration and stored for characterization.

Characterization of products

The X-ray-diffraction (XRD) patterns of samples were collected with a diffractometer (JEOL JDX–3500) with a monochromator under the following conditions: Cu*K*α radiation, 30 kV, 200 mA; scanning speed 2° 2θ min^{-1}; time constant 0.5 second.

Morphologies were observed with a scanning electron microscope, SEM (JEOL JSM–6300F) at 2–3 kV. This field-emission type of SEM enabled observation with very thin evaporation of platinum on the sample to avoid differential charging effects.

Infrared spectra were recorded by a Fourier transformation infrared spectrometer, FTIR (JASCO VALOR III) using diffuse reflectance infrared Fourier transform spectroscopy (DRIFTS) with 0.3 mass % of sample precipitate in KBr, under the conditions: accumulation, 64 times; resolution, 4 cm^{-1}; detector, TGS; range of wavenumbers, 400–4000 cm^{-1}.

The specific surface-area of product was determined by the N_2 gas adsorption method by a Quantasorb (Yuasa Ionics QS–13 with a cell QS–300 for low-value measurements).

Elemental compositions for the jarosite-type phases produced were determined by ICP–AES (SEIKO Co. Ltd., SPS 1200) after decomposition in 6 mol dm^{-3} HCl.

Results and Discussion

All XRD patterns indicate that the jarosite-group compounds synthesized do not contain crystalline by-products; this finding is shown for argentojarosite in Figure 1, jarosite in Figure 2, and ammoniojarosite in Figure 3. Cell parameters *a* and *c* of these jarosite compounds are in good agreement with the JCPDS data as listed in Table 1. As shown in Table 1, the composition was found mostly to be stoichiometric, except that some monovalent cations were slightly deficient: the mole ratios of Fe/S are close to 1.5 [the stoichiometric ratio in the formula, $MFe_3(SO_4)_2(OH)_6$] in all samples. Also, the colors of biological and chemical products were similar to those of the standards. There are distinctive IR absorbance frequencies of jarosite at 1190–1200 and 1080–1090 cm^{-1} (ν_3 mode of SO_4^{2-}), at 1010–1030 cm^{-1}

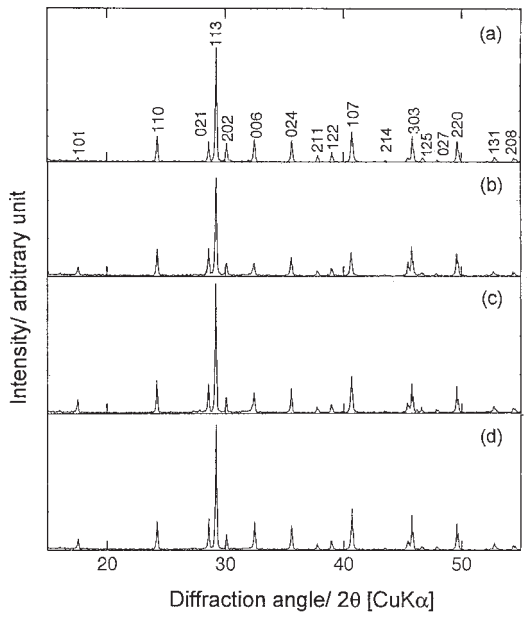

FIG. 1. XRD patterns of the argentojarosite produced. (a) standard, (b) biologically mediated product (Biological), (c) slow oxidation of Fe^{2+} ions by H_2O_2 (Chemical 1), and (d) rapid oxidation of Fe^{2+} ions by H_2O_2 (Chemical 2).

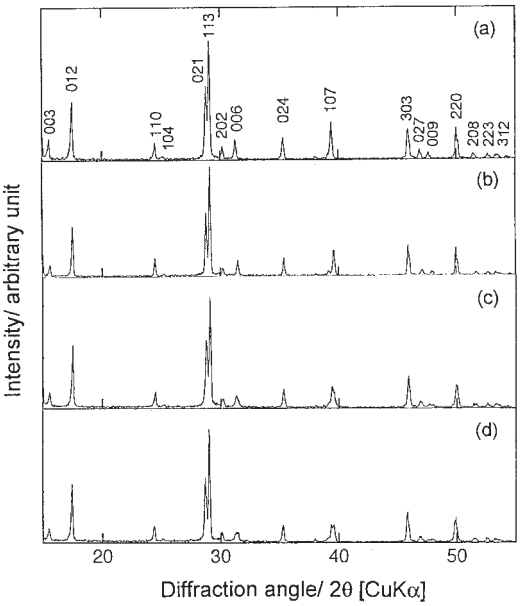

FIG. 2. XRD patterns of the jarosite produced. (a), (b), (c) and (d) are the same as in Figure 1.

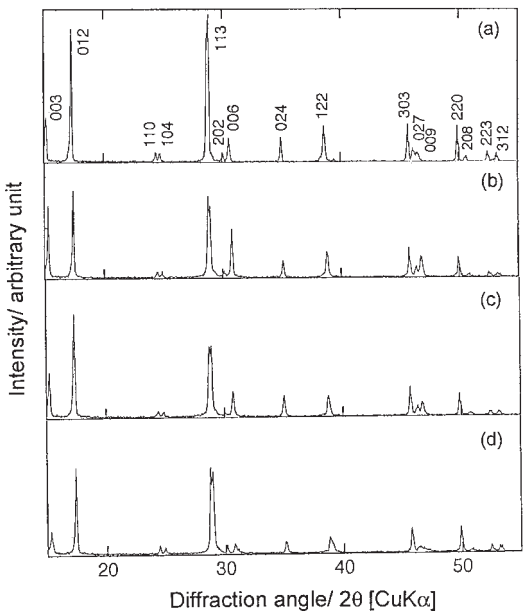

FIG. 3. XRD patterns of the ammoniojarosite produced. (a), (b), (c) and (d) are the same as in Figure 1.

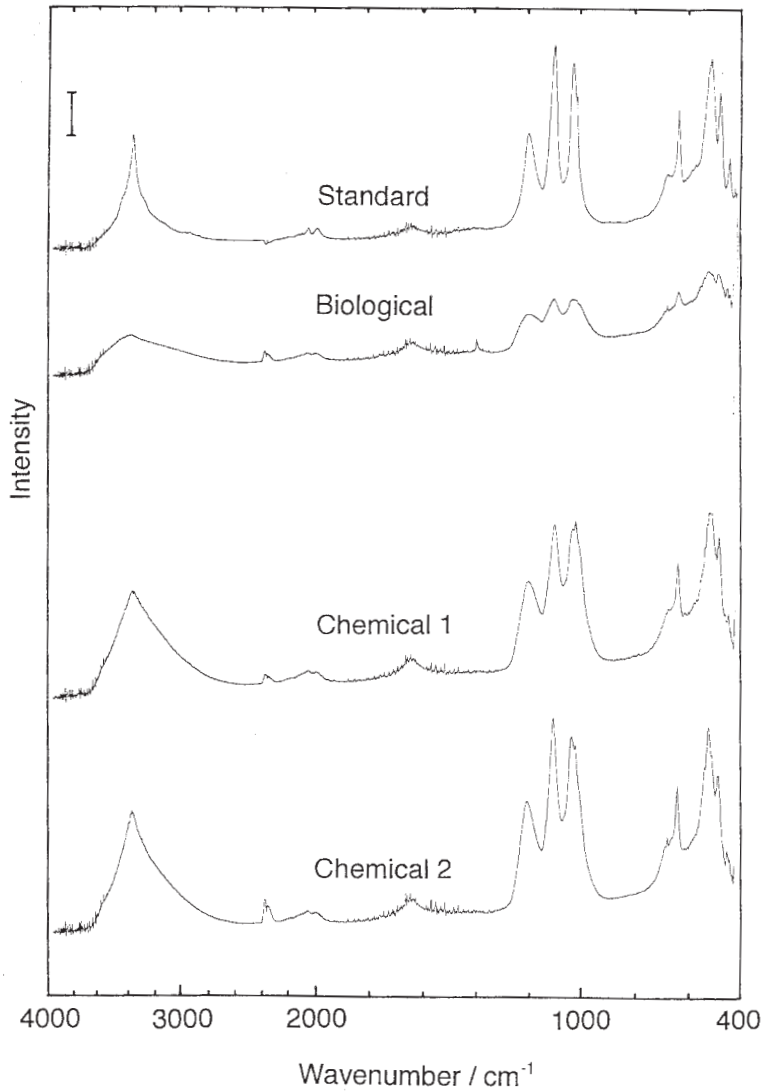

FIG. 4. FTIR spectra for the argentojarosite produced. Vertical bar indicates 1.2 Kubelka–Munk units for (a), one Kubelka–Munk unit for (b), (c) and (d). (a), (b), (c) and (d) are the same as in Figure 1.

(ν_1 mode of SO_4^{2-}), at 640–650 cm^{-1} (ν_4 mode of SO_4^{2-}), at 3300–3400 cm^{-1} (stretching mode of OH), at 1000–1010 cm^{-1} (σ mode of OH), and at 470–480 cm^{-1} (τ mode of OH) (Lazaroff *et al.* 1982, Tuovinen & Carlson 1979). For all products, these characteristic IR bands were observed by FTIR in agreement with those for standard jarosite-group compounds, though peak intensities of biologically mediated products are weaker than those of chemical products, as shown in Figures 4, 5 and 6. Peak intensities of the bands at 1190–1200 cm^{-1} and 1080–1090 cm^{-1} are linearly related to mass percentage of standard substances in KBr over the concentration range of two orders of magnitude with high correlation-coefficients, as shown in Figures 7a, b and c, showing that IR-derived purities can be estimated from this relationship (Sasaki *et al.* 1995). The order of IR purity was found to depend on the method of preparation, but to be independent of species, as follows: standard substances > chemical products 2 > chemical products 1 > biological products.

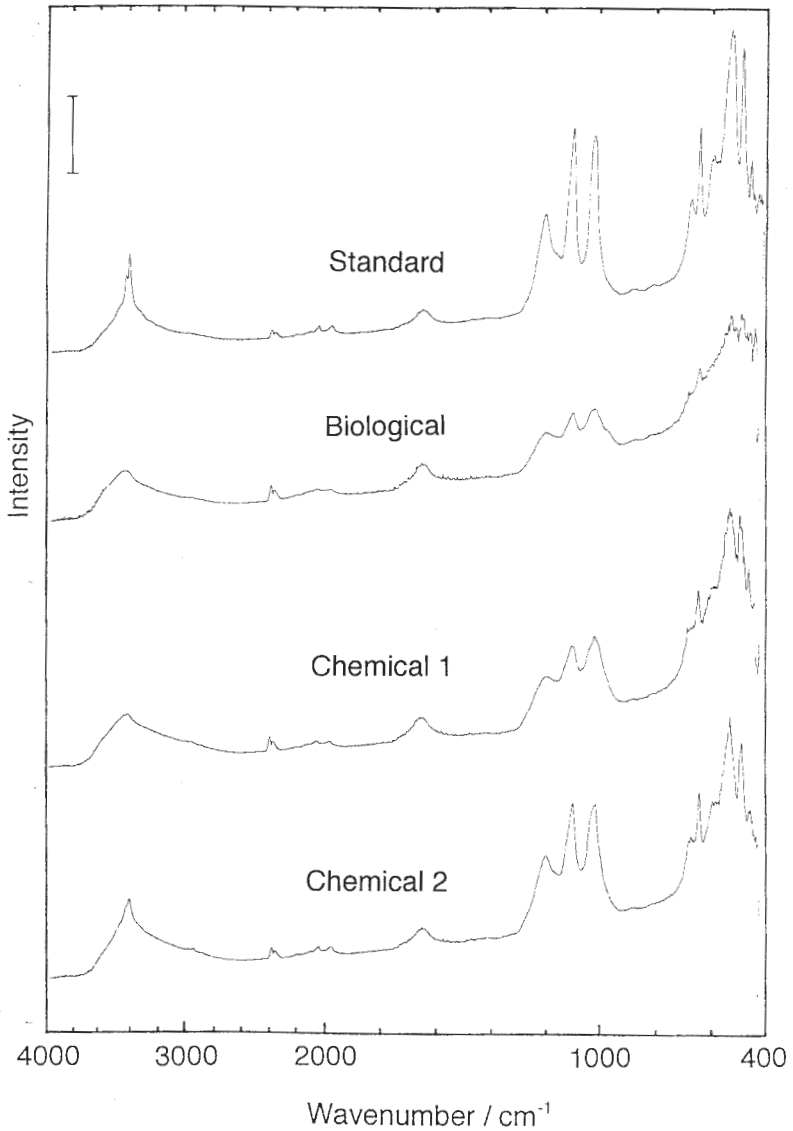

FIG. 5. FTIR spectra for the jarosite produced. Vertical bar indicates 1.2 Kubelka–Munk units for (a), one Kubelka–Munk unit for (b), (c) and (d). (a), (b), (c) and (d) are the same as in Figure 1.

The morphology of synthesized jarosite-group phases depends on the method of preparation. Generally, the jarosite-group phases formed by the same method showed similar morphology, though some differences were observed depending on which monovalent cations were involved. Common features from the different methods are summarized as follows: (1) crystals of the standard substances are small and irregular in shape, and not euhedral (Figs. 8a, 9a, 10a), (2) biological products consist of aggregates of submicroscopic crystal units (Figs. 8b, 9b, 10b), and (3) chemical products show distinct morphological characteristics: chemical products 2 (rapid) have large size-distributions and involve much larger particles (Figs. 8d, 9d, 10d) than chemical products 1 (slow), which are relatively uniform in crystal size (Figs. 8c, 9c, 10c).

The reason why the rate of H_2O_2 addition results in the above feature (3) cannot yet be explained com-

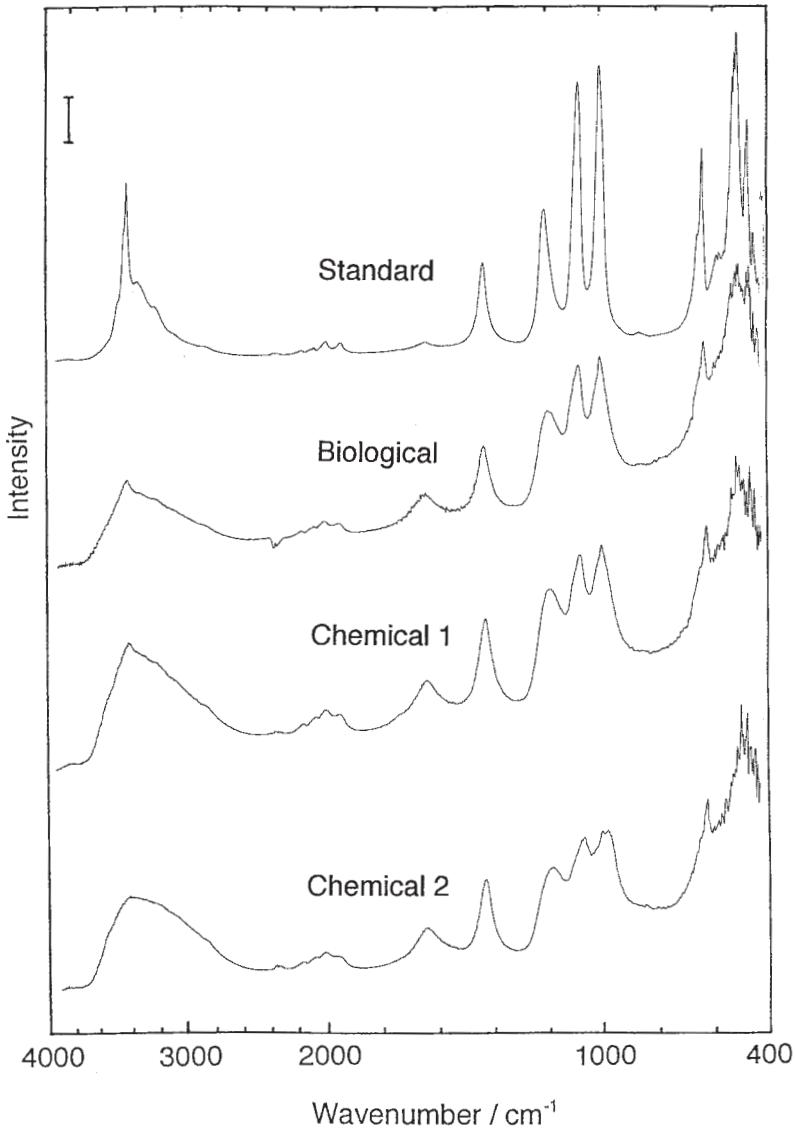

FIG. 6. FTIR spectra for the ammoniojarosite produced. Vertical bar indicates four Kubelka–Munk units for (a), one Kubelka–Munk unit for (b) and (c), and two Kubelka–Munk units for (d). (a), (b), (c) and (d) are the same as in Figure 1.

pletely, but it may be stated in a qualitative way as follows. On the oxidation of Fe^{2+} ions to Fe^{3+} ions, rapid addition of H_2O_2 causes rapid increase in the solution pH locally, according to the reaction

$$2\ Fe^{2+} + H_2O_2 + 2\ H^+ = 2\ Fe^{3+} + 2\ H_2O \quad \text{(chemical)} \quad [1]$$

and readily forms Fe^{3+} species such as $[Fe(H_2O)_5(OH)]^{2+}$ in addition to $[Fe(H_2O)_5(SO_4)]^+$, which is the precursor to jarosite-group phases (Sasaki *et al*. 1995). Rapid addition may lead to lower amounts of precursors or nuclei of jarosite-group phases at the initial stage. Lazaroff *et al*. (1982) described that polymers of Fe^{3+}-bearing octahedral species having hydroxyl and sulfate ligands could be precursors of both jarosite-group phases and amorphous hydroxysulfates, and that the incorporation of appropriate monovalent cations (M^+)

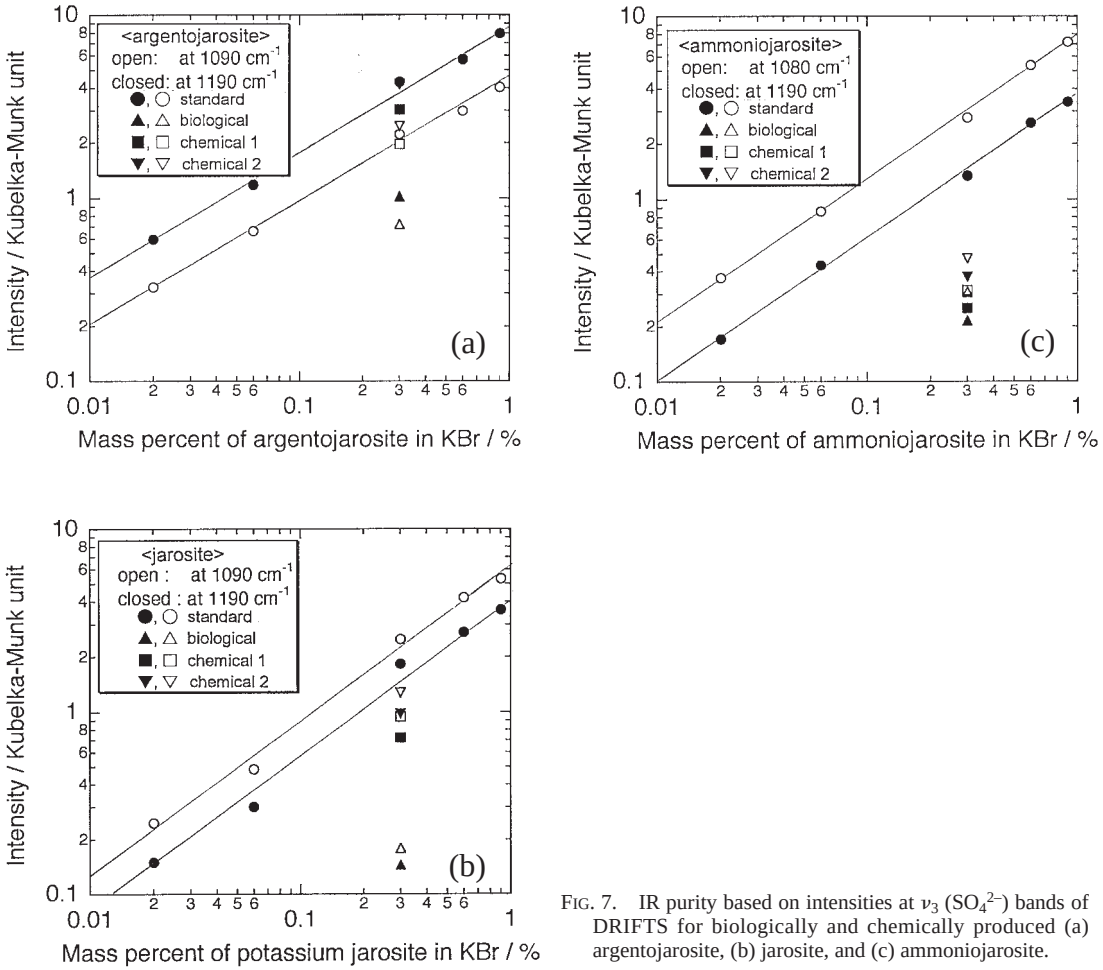

FIG. 7. IR purity based on intensities at ν_3 (SO_4^{2-}) bands of DRIFTS for biologically and chemically produced (a) argentojarosite, (b) jarosite, and (c) ammoniojarosite.

and additional sulfate ions leads to formation of a jarosite-group compound. The formation of Fe^{3+} polymers is promoted by the increase of pH, since normally Fe^{3+} ions polymerize by hydroxo-bridges. Formation of a jarosite-group phase decreases the solution's pH as expressed in eq. [2], which is favorable to further formation of jarosite and not of amorphous species such as Fe^{3+}-oxyhydroxides.

$$M^+ + 3\ Fe^{3+} + 2\ HSO_4^- + 6\ H_2O = M Fe_3(SO_4)_2(OH)_6 + 8\ H^+ \text{ (chemical)} \quad [2]$$

Thus, fewer precursor particles or nuclei of jarosite and various types of Fe^{3+} species, which eventually dissolve and contribute to the ripening of crystals (Ostwald ripening), may result in the large size-distribution. On the contrary, the slow addition of H_2O_2 does not change the solution's pH very much, that is, the pH is balanced by a slow increase due to the oxidation of Fe^{2+} (eq. [1]) and a slow decrease due to the formation of a jarosite-type compound (eq. [2]). This situation avoids the formation of different types of Fe^{3+} species, leading to the formation of many small precursor particles or nuclei of a jarosite-type compound having more uniform size than those from rapid addition of H_2O_2.

The biological oxidation of Fe^{2+} ions proceeds as in eq. [3] and is much slower than the chemical oxidation by slow addition of H_2O_2 carried out in the present work.

$$2\ Fe^{2+} + 1/2\ O_2 + 2\ H^+ = 2\ Fe^{3+} + H_2O \text{ (biological)} \quad [3]$$

In addition, extracellular substances, such as polysaccharide (Sadowski 1999), are produced during cellular metabolism, and they affect the surface free energy of crystal nuclei of a jarosite-group phase. Usually, crystal growth is inhibited in biologically mediated systems. Therefore, the biological products often occur in the

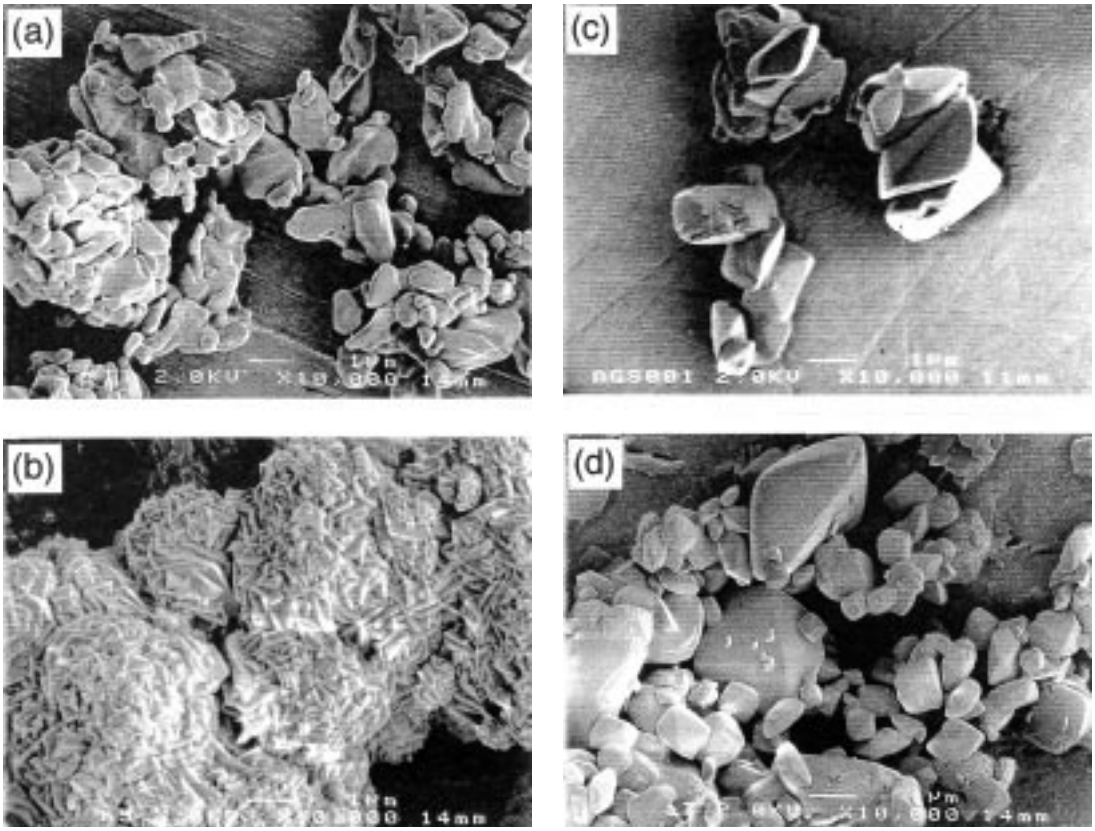

FIG. 8. SEM images of the argentojarosite produced. (a), (b), (c) and (d) are the same as in Figure 1. Magnification is the same for all images. Scale bar: 1 μm.

form of small crystal units that bind to each other, and they are not as euhedral as the chemical products 1.

Morphological features from the monovalent cations involved are summarized as follows. As reported previously (Sasaki *et al.* 1995), argentojarosite is commonly euhedral, except for the standard substance (Fig. 8a); the biological product consists of "aggregates" of many square pieces with sharp edges and submicrometric microstructures (Fig. 8b), whereas the chemical products consist of several micrometric particles that form pyramidal rhombs with smooth surfaces and separate from each other (Figs. 8c, d). In contrast to argentojarosite, jarosite consists mostly of round and granular particles, and sharp edges are not developed (Figs. 9b, c and d). Akai *et al.* (1999) reported that the shape of crystals of natural jarosite at the Gunma iron mine, Japan, which is abiotic in origin, is similar to that in Figures 8d and 10d, and their sizes are much larger than the present results, though the chemical composition of the natural jarosite is not reported. The differences from the present results may be due to the time and conditions of crystallization. However, the tendency of aggregation and particle-size distribution are very similar to those of argentojarosite when prepared by the same method. Ammoniojarosite looks like aggregates of near-cubic particles (Figs. 10b, c and d), though the sizes of chemical product 2 are exceptionally large (Fig. 10d). Apparently, morphologies of biological product (Fig. 10b) and chemical product 1 (Fig. 10c) are similar, but the planar facets are more developed in the latter than the former.

The above differences are considered to be caused by the rate of formation of the jarosite compounds, depending on which monovalent cations are involved. Figure 11 shows the changes in the concentration of Fe and S species and pH during experiments in Method IV. XRD patterns of products confirmed the formation of single-phase argentojarosite, jarosite and ammoniojarosite. It should be noted again that in this method, Fe^{3+} ions were supplied as a sulfate at the same initial concentration and not by the oxidation of Fe^{2+} ions. It is clear from Figure 11 that the rate of formation of a jarosite-group phase is higher in the order argento-

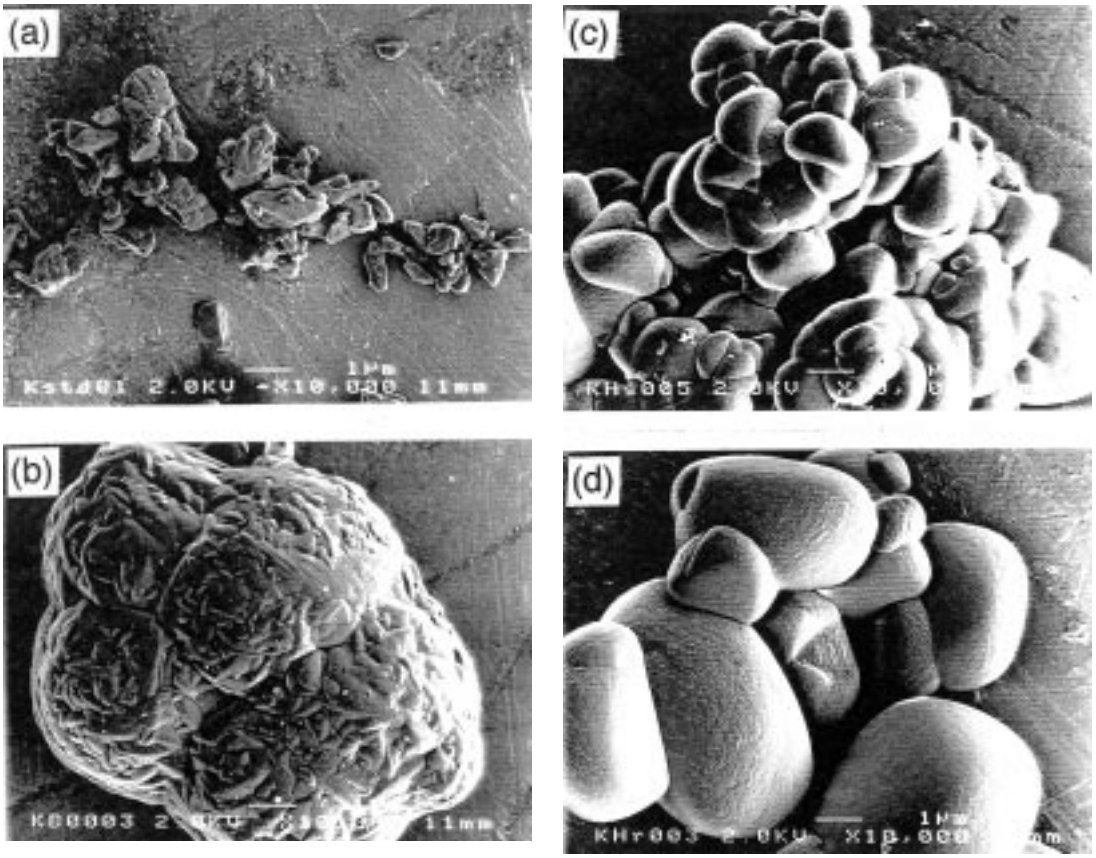

FIG. 9. SEM images of the jarosite produced. (a), (b), (c) and (d) are the same as in Figure 1. Magnification is the same for all images. Scale bar: 1 μm.

jarosite > jarosite > ammoniojarosite. Ivarson *et al.* (1979) have reported that in the biologically mediated formation of jarosite-group compounds by *T. ferrooxidans*, jarosite is formed more quickly than ammoniojarosite under the same conditions. The slow rate of formation of ammoniojarosite may lead to the formation by the chemical method of aggregates with many small crystals, similar to the biological products. This phenomenon does not occur in the formation of argentojarosite and jarosite, because the rate of formation by the slow addition of H_2O_2 is sufficiently faster than the biological oxidation method by *T. ferrooxidans*.

CONCLUSIONS

Argentojarosite, jarosite and ammoniojarosite were synthesized by supplying Fe^{3+} ions in three different ways: the biological oxidation of Fe^{2+} ions by *T. ferrooxidans*, the chemical oxidation of Fe^{2+} ions by slow addition of H_2O_2, and the chemical oxidation by rapid addition of H_2O_2. They were characterized by XRD, FTIR, chemical analysis and SEM, and morphological features were discussed compared with those formed by the hydrothermal method (standard substances). Conclusions are summarized as follows.

(1) XRD patterns indicate that synthesized jarosite-group compounds do not contain crystalline by-products. The order of IR purity was found to be dependent on the method of preparation and to be independent of the jarosite-group species; the order was standard substances > chemical products 2 (by rapid oxidation of Fe^{2+} ions) > chemical products 1 (by slow oxidation of Fe^{2+} ions) > biological products.

(2) Two main factors were found to affect the morphology, the method and rate of supply of Fe^{3+} ions, and the nature of the monovalent cation, which determines, the intrinsic rate of formation under given conditions.

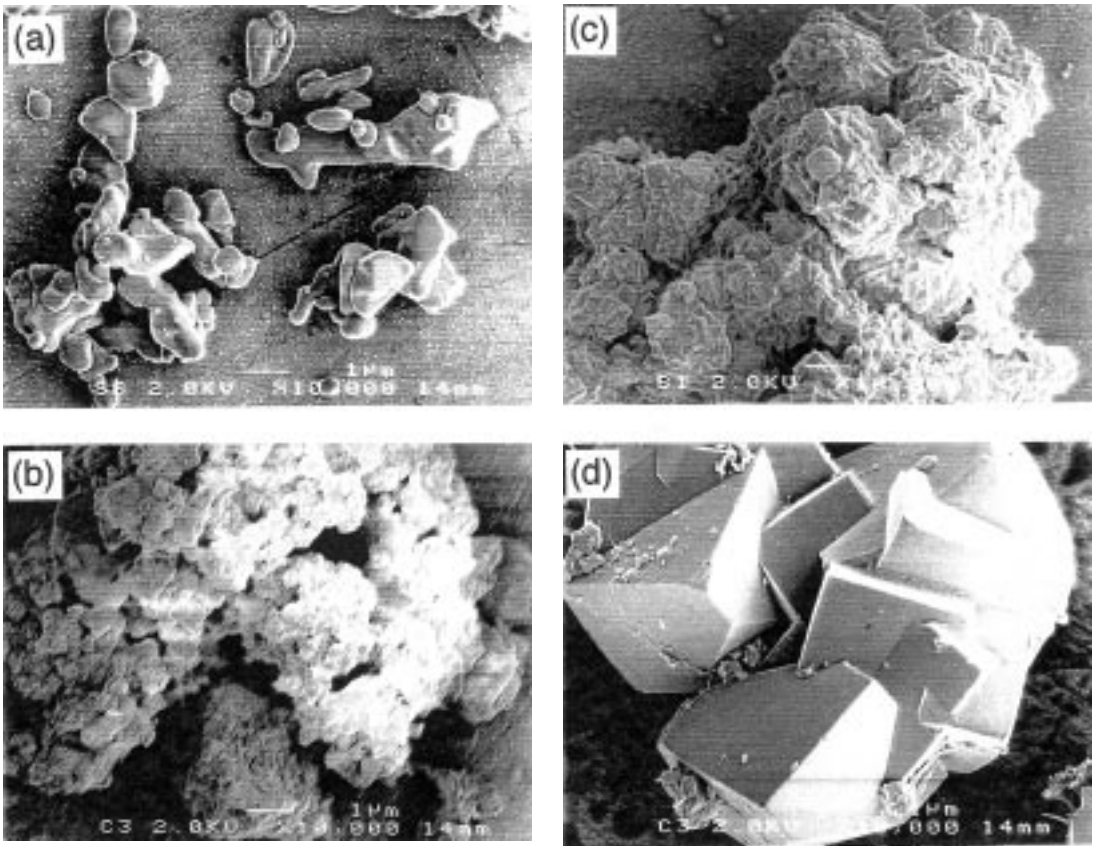

FIG. 10. SEM images of produced ammoniojarosite. (a), (b), (c) and (d) are the same as in Figure 1. Magnification is the same for all images. Scale bar: 1 μm.

(3) Where Fe^{3+} ions were present in the system from the beginning, the order of rate of formation was confirmed to be argentojarosite > jarosite > ammoniojarosite at 30°C.

(4) The morphological features of jarosite-group compounds formed by the biological method were particularly distinguishable owing to the effect of extracellular substances.

ACKNOWLEDGEMENTS

We deeply appreciate the help of Dr. J.E. Dutrizac at CANMET in Canada, for supplying standard jarosite-group compounds, and also thank to Prof. Luke L.Y. Chang at University of Maryland and Robert F. Martin, McGill University, for comments on this manuscript. This work was partly supported by Hayashi Memorial Foundation for Female Natural Scientists and Arai Science and Technology Foundation.

REFERENCES

AKAI, J., AKAI, K., ITO, M., NAKANO, S., MAKI, Y. & SASAGAWA, I. (1999): Biologically localized iron ore at Gunma iron mine, Japan. *Am. Mineral.* **84**, 171-182.

BIGHAM, J.M. (1994): Mineralogy of ochre deposits formed by sulfide oxidation. *In* Environmental Geochemistry of Sulfide Mine-Wastes (J.L. Jambor & D.W. Blowes, eds.). *Mineral. Assoc. Can., Short Course* **22**, 103-132.

DUTRIZAC, J.E. & KAIMAN, S. (1976): Synthesis and properties of jarosite-type compounds. *Can. Mineral.* **14**, 151-158.

GRISHIN, S.I., BIGHAM, J.M. & TUOVINEN, O.H. (1988): Characterization of jarosite formed upon bacterial oxidation of ferrous sulfate in a packed bed reactor. *Appl. Environ. Microbiol.* **54**, 3101- 3106.

IVARSON, K.C., ROSS, G.J. & MILES, N.M. (1979): The microbiological formation of basic ferric sulfates. II. Crystalliza-

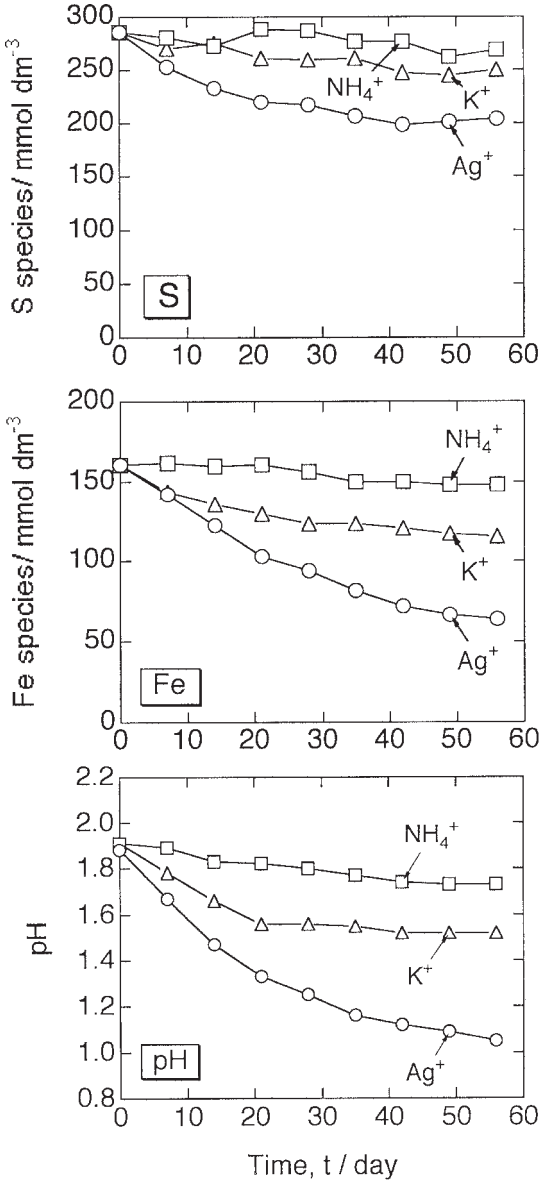

FIG. 11. Changes in S, Fe species and pH during jarosite formation in Method IV.

tion in presence of potassium-, ammonium-, and sodium-salts. *Soil Sci. Soc. Am. J.* **43**, 908-912.

KOIWASAKI, K., HONBO, Y., TAZAKI, K. & MORI, T. (1993): Formation of jarosite and ammoniojarosite by *Thiobacillus ferrooxidans*. *Chikyu Kagaku* **47**, 493-506 (in Japanese, with English abstr.).

LAZAROFF, N., MELANSON, L., LEWIS, E., SANTORO, N. & PUESCHEL, C. (1985): Scanning electron microscopy and infrared spectroscopy of iron sediments formed by *Thiobacillus ferrooxidans*. *Geomicrobiol. J.* **4**(3), 231-268.

_____, SIGAL, W. & WASSERMAN, A. (1982): Iron oxidation and precipitation of ferric hydroxysulfates by resting *Thiobacillus ferrooxidans* cells. *Appl. Environ. Microbiol.* **43**, 924-938.

NORDSTROM, D.K. (1982): Aqueous pyrite oxidation and the consequent formation of secondary iron minerals. *In* Acid Sulfate Weathering (J.A. Kittrick, D.S. Fanning, L.R. Hossner, D.M. Kral & S. Hawkins, eds.). *Soil Science Soc. Am., Spec. Publ.* **10**, 37-56.

SADOWSKI, Z. (1999): Adhesion of microorganism cells and jarosite particles on the mineral surface. *In* Biohydrometallurgy and the Environment toward the Mining of the 21st Century (R. Amils & A. Ballester, eds.). Elsevier, New York, N.Y. (393-398).

SASAKI, K. (1997): Morphological characterization of jarosite groups formed through mediation of *Thiobacillus ferrooxidans*. *J. Mineral. Soc. Japan* **26**, 47-50 (in Japanese, with English abstr.).

_____, TSUNEKAWA, M. & KONNO, H. (1995): Characterization of argentojarosite formed from biologically oxidized Fe^{3+} ions. *Can. Mineral.* **33**, 1311-1319.

_____, _____, _____, HIRAJIMA, T. & TAKAMORI, T. (1993): Leaching behavior and surface characterization of pyrite in bacterial leaching with *Thiobacillus ferrooxidans*. *Shigen-to-Sozai* **109**, 29-35 (in Japanese, with English abstr.).

SILVERMAN, M.P.& LUNDGREN, D.G. (1959): Studies on the chemoautotrophic iron bacterium *Ferrobacillus ferrooxidans.* 1. An improved medium and a harvesting procedure for securing high cell yield. *J. Bacteriol.* **77**, 642-647.

SINGER, P.C.& STUMM, W. (1970): Acid mine drainage: the rate-determining step. *Science* **167**, 1121-1123.

SUGIO,T., TANO, T. & IMAI, K. (1981): Isolation and some properties of silver ion-resistant iron-oxidizing bacterium *Thiobacillus ferrooxidans*. *Agric. Biol. Chem.* **45**, 2037-2051.

TAYLOR, B.E., WHEELER, M.C.& NORDSTROM, D.K. (1984): Isotope composition of sulphate in acid mine drainage as measure of bacterial oxidation. *Nature* **308**, 538-541.

TUOVINEN, O.H. & CARLSON, L. (1979): Jarosite in cultures of iron-oxidizing *Thiobacilli*. *Geomicrobiol. J.* **1**(3), 205-210.

VERATI, C., DONATO, DE P., PRIEUR, D. & LANCELOT, J. (1999): Evidence of bacterial activity from micrometer-scale layer analyses of black-smoker sulfide structures (Pito Seamount Site, Easter microplate). *Chem. Geol.* **158**, 257-269.

Received August 10, 1999, revised manuscript accepted January 26, 2000.